Published in final edited form as:
Restor Neurol Neurosci. 2010 ; 28(2): . doi:10.3233/RNN-2010-0488.

Adult plasticity of spatiotemporal receptive fields of multisensory superior colliculus neurons following early visual deprivation

David W. Royal[a,*], **Juliane Krueger**[a], **Matthew C. Fister**[b], and **Mark T. Wallace**[a,b]
[a]Kennedy Center for Research on Human Development, Nashville, Tennessee, USA
[b]Department of Hearing and Speech Sciences, Vanderbilt University, Nashville, Tennessee, USA

Abstract

Purpose—Previous work has established that the integrative capacity of multisensory neurons in the superior colliculus (SC) matures over a protracted period of postnatal life (Wallace and Stein, 1997), and that the development of normal patterns of multisensory integration depends critically on early sensory experience (Wallace et al., 2004). Although these studies demonstrated the importance of early sensory experience in the creation of mature multisensory circuits, it remains unknown whether the reestablishment of sensory experience in adulthood can reverse these effects and restore integrative capacity.

Methods—The current study tested this hypothesis in cats that were reared in absolute darkness until adulthood and then returned to a normal housing environment for an equivalent period of time. Single unit extracellular recordings targeted multisensory neurons in the deep layers of the SC, and analyses were focused on both conventional measures of multisensory integration and on more recently developed methods designed to characterize spatiotemporal receptive fields (STRF).

Results—Analysis of the STRF structure and integrative capacity of multisensory SC neurons revealed significant modifications in the temporal response dynamics of multisensory responses (e.g., discharge durations, peak firing rates, and mean firing rates), as well as significant changes in rates of spontaneous activation and degrees of multisensory integration.

Conclusions—These results emphasize the importance of early sensory experience in the establishment of normal multisensory processing architecture and highlight the limited plastic potential of adult multisensory circuits.

Keywords

superior colliculus; multimodal; cat; cross-modal; experiential plasticity

1. Introduction

The natural world can be described as a never-ending stream of stimuli that change rapidly across the dimensions of space and time. The spatiotemporal complexities inherent to these real world stimuli continually challenge the processing capabilities of the nervous system. One feature of the real world and the brains that have evolved to live in this world is that individual stimulus events and features are often specified by energies contained within

[*]Corresponding author: David W. Royal, Vanderbilt University, 7110 MRB III, Nashville, TN 37232, USA. Tel.: +1 615 936 7104; Fax: +1 615 936 3745; david.royal@vanderbilt.edu.

multiple sensory systems. For example, a bouncing ball is defined both by the change of visual direction as well as by the sound generated by the collision of the ball with the substrate. These redundant multisensory signals are closely linked in the spatiotemporal domain, since they are likely to share a common spatial and temporal origin. Not surprisingly, given the inherent utility of these multisensory cues for "binding" unitary events (and thus increasing their detectability and salience), brain structures have evolved that are specialized for the processing and integration of multisensory information cues. One of the best studied of these structures is the superior colliculus (SC), a midbrain nucleus that receives convergent visual, auditory and somatosensory inputs (Calvert, 2004; Meredith and Stein, 1986; Stein and Meredith, 1993; Wallace et al., 1993). The SC is spatiotopically ordered, and plays a central role in the transformation of (multi)sensory signals into motor commands to move the eyes, ears and head toward a stimulus of interest.

As a result of these convergent sensory inputs, a large population of multisensory neurons, which respond to or are influenced by two or more sensory modalities, is found in the SC. Like multisensory neurons in other brain structures, those in the SC actively integrate their different sensory inputs to give rise to responses that often differ significantly from both of the constituent unisensory responses, as well as from that predicted by their simple summation (Carriere et al., 2008; Stein and Wallace, 1996; Wallace et al., 1992). Prior work has shown that both the sign (i.e., enhancement or depression) and magnitude of these integrated responses depend upon the nature of the combined stimuli and on their relationships to one another; stimuli that are in close spatial and temporal proximity, and that are weakly effective when presented alone, typically result in large response enhancements when combined (Meredith and Stein, 1986; Wallace et al., 1992). Although traditionally studied in isolation, the spatial, temporal, and inverse effectiveness principles of multisensory integration have recently been shown to operate in a synergistic fashion (Carriere et al., 2008; Royal et al., 2009).

In the best-studied model species, the cat, the SC's organization and multisensory processing capabilities have been shown to be remarkably plastic during a protracted period of postnatal life. Most importantly, visual experience appears to be critical in this developmental process, since animals raised in absolute darkness fail to develop normal multisensory integrative characteristics (Carriere et al., 2007; Wallace et al., 2004; Wallace and Stein, 2007). Furthermore, recent work has shown that the spatial and temporal constraints of this developmental process are remarkably malleable, being strongly shaped by the statistics of the early sensory world (Carriere et al., 2008). For example, raising an animal in an environment in which visual and auditory cues are presented simultaneously but from different spatial locations results in an integrative circuitry "tuned" to this spatial disparity. Nonetheless, despite these studies, it remains unknown whether the introduction of normal sensory experience in adulthood is sufficient to restore normal spatiotemporal response dynamics and integrative characteristics to multisensory SC neurons. In the current study, we sought to address these issues by characterizing the spatiotemporal receptive fields (STRFs) and integrative capacities of multisensory SC neurons recorded from adult cats that were reared in absolute darkness until adulthood and then returned to a normal housing environment as adults for an equivalent period of time (i.e., 6 mos. or longer).

2. Methods

2.1. Experimental groups and rearing conditions

Experiments were conducted on two groups of adult (> 6 months of age) cats; animals reared under normal lighting and housing conditions (n = 4), and animals that were born and raised in complete darkness for 6 months and then transferred to standard lighted housing for a minimum of 6 additional months (n = 2). For ease of description, these animals will be

referred to hereafter as NR (i.e., normally-reared) and DR+ (i.e., dark-reared plus adult visual experience), respectively. Daily care and routine veterinary procedures in the dark housing environment were carried out using binocular infrared goggles (illuminator $\lambda = 920$ nm – well outside of the visible range of the cat visual system). Additional infrared surveillance systems allowed for continuous monitoring from an adjacent room, and the output of these cameras was stored on a digital video recorder for archival purposes.

2.2. General procedures

Once cats lived in a standard housing environment for at least 6 month, they were implanted (see below) to allow for neurophysiological recording experiments to commence. Experiments were comprised of extracellular single-unit recordings from visual/auditory multisensory superior colliculus (SC) neurons. All experiments took place in anesthetized and paralyzed semichronic preparation at a frequency of once per week. All surgical and recording procedures were performed in compliance with the *Guide for the Care and Use of Laboratory Animals* (National Institutes of Health publication number 91-3207) at Vanderbilt University Medical Center, which is accredited by the American Association for Accreditation of Laboratory Animal Care.

2.3. Implantation and recording procedure

Prior to implantation of the hardware necessary for these recording experiments, anesthesia was induced with a combination of ketamine hydrochloride (20 mg/kg; im) and acepromazine maleate (0.04mg/kg; im). Animals were then transported to a surgical suite, intubated, artificially respired and placed on inhalation isoflurane for maintenance of anesthesia. Vital signs including heart rate, blood pressure, core temperature, and expiratory CO2 were continuously recorded and monitored (VetSpecs model VSM7), and were regulated so as to maintain a deep and stable plane of anesthesia. A craniotomy was then made in the skull to enable access to the superior colliculus, and a stainless steel chamber and head holder were affixed to the skull utilizing stainless steel bone screws and orthopedic cement. This design ensured a recumbent positioning of the animal during recording procedures without obstructing its visual or auditory fields. Preoperative and postoperative care (e.g., administration of analgesics and antibiotics) was provided in close consultation with the veterinary staff. At least one week of recovery was permitted before the first recording session took place.

For recording experiments, anesthesia was induced with ketamine hydrochloride (20 mg/kg; im) and acepromazine maleate (0.04 mg/kg; im), and was maintained throughout the procedure with an infusion of ketamine (5 mg/kg/hr; a rate sufficient to maintain a stable plane of anesthesia) administered intravenously through the saphenous vein. To eliminate any prolonged pressure points, the animal's natural sitting position was recreated and ensured through the head-holding system. Artificial respiration was begun and was followed with the administration of the neuromuscular blocking agent, pancuronium bromide (0.1 mg/kg/hr; im), which was administered in order to prevent ocular drift. Recording microelectrodes (parylene-insulated tungsten, $Z = 3–6\ M\Omega$ at 1 kHz) were advanced into the SC using a mechanical microdrive until a multisensory neuron was isolated (minimum signal : noise 3:1). Neural activity was amplified and recorded through a Plexon 16 channel MAP system, which also stored the unprocessed data for subsequent on- and offline analyses.

2.4. Search strategy and stimulus presentation

In order to isolate multisensory neurons, a battery of search stimuli (Carriere et al., 2007; Carriere et al., 2008; Perrault et al., 2003; Wallace et al., 2006; Wallace et al., 1997; Wallace et al., 1998) was used to determine the neurons' sensory responsive profile and to streamline

subsequent quantitative testing. Visual stimuli consisted of 100 ms duration flashes of a single light-emitting diode (LED) and were presented monocularly to the eye contralateral to the recording electrode (the ipsilateral eye was occluded). Auditory stimuli consisted of 100 ms broadband (20 Hz to 20 kHz) noise bursts (50.6 to 70 dB sound pressure level on 45 dB SPL background; A-weighted) that were delivered through a single freely positionable speaker. The location(s) of the LED and speaker were positioned by hand and affixed to a translucent screen after an initial qualitative determination of the borders of the visual and auditory receptive fields(s) (RFs). These RF borders were mapped using conventional methods (Wallace, Meredith, et al., 1992; Wallace et al., 2004). Stimulus conditions [visual (V), auditory (A), multisensory (VA)] were randomly interleaved until a minimum of 15 trials was collected for each condition. Consecutive stimulus presentations were separated by not fewer than six seconds to avoid response habituation. Each neuron was tested with the identical stimulus set at numerous locations (typically at 5–10° increments across the RF's widest aspect) along a single plane of azimuth in order to construct its STRF (Fig. 1). Plotting spike density functions (SDFs) in this way helped reveal a neuron's response dynamics across the joint dimensions of space and time.

2.5. Data acquisition and data analysis

A custom-build PC-based real-time data acquisition system managed the structure of the stimulus delivery. The Plexon system recorded and stored the spike data. Data analysis was performed offline and employed the Plexon OfflineSorter, NeuroExplorer, and customized MATLAB scripts. After a multisensory neuron was isolated and its receptive fields were mapped, its STRF architecture and integrative capacity was tested by pairing weakly effective spatially and temporally coincident visual and auditory stimuli, which have been shown to maximize the potential for multisensory interaction (Meredith and Stein, 1986; Perrault et al., 2003). Weak stimuli are operationally defined as those that elicit a slightly suprathreshold (i.e. statistically significant from spontaneous firing) response.

Peristimulus time histograms (PSTHs) and collapsed SDFs were used to describe the neuron's response profile to any given condition. SDFs were computed by convolving the spike train from each trial for any given condition and location with a function akin to a postsynaptic potential specified by the time constant for the growth phase (τ_g) and the time constant for the decay (τ_d):

$$R(t)=[1-exp(-t/\tau_g)]exp(-t/\tau_g)$$

Values of 1 ms and 20 ms were chosen for τ_g and τ_d, respectively; based upon previous established physiological records from excitatory synapses (Kim and Connors, 1993; Mason et al., 1991; Sayer et al., 1990). The mean firing rate of the neuron during the 500 ms prior to stimulus onset was calculated to give the neuron's background firing rate. SDFs were then thresholded at two standard deviations above their respective baselines in order to delimit the evoked responses (i.e., a suprathreshold response lasting at least 30 consecutive milliseconds with a latency shorter than 30 ms for the auditory condition and 100 ms for the visual condition). Single units failing to meet these criteria to both visual and auditory stimulation were excluded from additional investigation. Mean stimulus-evoked responses were computed by calculating the mean number of spikes elicited between response onset and offset. Response duration was determined by subtracting the time of response onset from the time of response offset, and peak firing rate was determined by finding the maximum firing rate during the interval spanning response onset and offset. A Student's *t*-test was used to evaluate significant differences in evoked response latencies, response durations, mean firing rates, and peak firing rates between the multisensory and the predicted multisensory (linear addition of the visual and auditory evoked responses)

stimulus conditions. NR and DR+ multisensory stimulus evoked latencies, response durations and peak firing rates were compared using a *t*-test.

2.6. Multisensory interactive analyses

Stimulus-evoked responses collected during multisensory trials were compared to the responses of the most effective unisensory condition and were quantified using the *interactive index*:

$$I=[(M-U)/U]\times 100$$

in which *I* represents the multisensory interactive product, *M* is the multisensory response, and *U* is the response of the most effective unisensory condition (Meredith and Stein, 1983, 1986). Statistical comparison of the mean-evoked responses of the multisensory and the best unisensory condition was done by utilizing a two-tailed paired Student's *t*-test. *Mean statistical contrast* or *multisensory contrast* was a second measure employed to analyze the multisensory response. It evaluates the multisensory response as a function of the predicted addition of the two unisensory responses using the formula:

$$\sum[(SA-A)-(V-VA)]/n$$

where SA is the spontaneous activity, A is the auditory response, V is the visual response, VA is the multisensory response, and n is the number of trials. The model presumes independence between visual and auditory inputs and employs additive factors logic to differentiate between subadditive (contrast < 0) and superadditive (contrast > 0) modes of response (Perrault et al., 2003, 2005; Stanford et al., 2005). Significant differences from a contrast value of zero were tested via a *t*-test.

2.7. Spatial receptive field analyses

Mean stimulus-evoked firing rates were normalized with the highest stimulus-evoked responses from all tested locations and conditions for each recorded neuron, giving a range of 0.0 to 1.0. Visual, auditory, and multisensory spatial receptive fields (SRFs) were then constructed for each neuron by arranging the normalized firing rates in a matrix (one matrix per stimulus condition) such that the relative location within the matrix corresponded to the spatial location of the evoking stimulus or stimuli (Figs 2–3, right column). The predicted multisensory SRF was computed by linear addition of the visual and auditory SRFs. To enhance visualization of SRF architecture, the SRF structure of each condition was interpolated in two dimensions using the method of cubic splines.

3. Results

A total of 76 sensory responsive neurons were isolated in electrode penetrations that targeted the multisensory layers (i.e., stratum griseum intermediale and below) of the SC in normal-reared cats ($n = 45$) and those that had been dark-reared and then returned to normal lighting conditions ($n = 31$). Of the 45 SC neurons recorded from NR animals, 22 were stimulus-driven visual-auditory multisensory neurons, the focus of the current study. The remaining population of neurons were either unisensory visual ($n = 17$) or unisensory auditory ($n = 6$). Of the 31 SC neurons recorded from DR+ animals, 23 were stimulus-driven visual-auditory multisensory neurons, while the remaining neurons were either unisensory visual ($n = 4$) or unisensory auditory ($n = 4$). Consistent with previous reports, the receptive fields of multisensory SC neurons from NR cats typically exhibited a high degree of spatial overlap,

and showed marked response heterogeneities within these receptive fields (Meredith and Stein 1986;Wallace et al., 1993;Wallace and Stein 1997). The receptive fields of multisensory neurons in the DR+ animals were qualitatively larger than in their NR counterparts, but still demonstrated a similarly high degree of spatial overlap.

3.1. Spatiotemporal receptive field (STRF) architecture of SC multisensory neurons differs between normally-reared (NR) and dark-reared animals with adult visual experience (DR+)

In order to examine the STRF structure of multisensory SC neurons in the two populations, visual and auditory stimuli that differed only in their spatial location along a single plane of azimuth were presented (see Fig. 1). The component visual and auditory stimuli for these multisensory combinations were always presented at the same location (i.e., spatial coincidence). With this stimulus structure, a first-order approximation of the STRFs of these neurons in the visual, auditory and multisensory (i.e., visual-auditory) domains was constructed (Figs 1 and 2). In each of the 22 visual-auditory neurons examined from NR animals, the STRF architecture consisted of multiple regions of elevated response (i.e., “hot spots”) surrounded by regions of lesser response (Fig. 2). In nearly all of these neurons (n = 20; 87%), superadditive and subadditive multisensory interactions were seen across multiple stimulus locations (Fig. 2), suggesting that the multisensory SC neurons of NR animals express a range of integrative capacities, a finding in strong concordance with previous studies (Meredith and Stein 1986; Wallace et al., 1993;Wallace and Stein 1997).

These spatiotemporal patterns of activation are in stark contrast to the results of similar analyses performed on data from the DR+ population. For example, in each of the 23 visual-auditory neurons from the DR+ animals, unisensory and multisensory responses exhibited striking similarities in their temporal response profiles as a function of stimulus location. In virtually every example, the STRF architecture consisted of a single position of elevated response surrounded by regions of lesser response (Fig. 3). The most dramatic finding was that for every neuron examined, the multisensory STRFs were remarkably similar to the linear summation of the component unisensory STRFs, differing significantly from the results seen in the NR population, and suggesting a compromised capacity for multisensory integration (Fig. 3).

3.2. The temporal response dynamics of SC multisensory neurons differ between normally-reared (NR) and dark-reared animals with adult visual experience (DR+)

In an effort to better characterize this spatiotemporal structure of the receptive fields in these two populations, the temporal dynamics of the unisensory and multisensory stimulus evoked responses were investigated by determining response latencies, response durations, and peak firing rates. In the NR population, peak firing rates and mean firing rates were significantly greater in the multisensory condition (82 ± 18 Hz and 42 ± 17 Hz, respectively) compared to the response predicted by a simple linear summation of the constituent unisensory responses (51 ± 23 Hz and 32 ± 16 Hz, respectively) (peak: $p < 0.01$; mean: $p < 0.01$). Although there was significant latency variability between individual NR neurons and across spatial locations for the same NR neuron (e.g., see Fig. 2), on average, multisensory response latencies (51 ± 8 ms) did not differ significantly from the predicted multisensory response latencies (54 ± 12 ms) ($p > 0.05$), with this value generally being dictated by the fastest arriving input (i.e., auditory). Finally, while the mean multisensory response duration (349 ± 95 ms) trended higher than the mean predicted multisensory response duration (315 ± 87 ms), the difference failed to reach significance ($p > 0.05$).

Analyses of the temporal response dynamics characteristic of DR+ multisensory SC neurons revealed a different pattern. Comparisons of peak and mean firing rates across conditions revealed that the actual multisensory responses (125 ± 47 Hz and 77 ± 35 Hz, respectively)

were not significantly different from the predicted multisensory responses (132± 51 Hz and 83 ± 36 Hz, respectively) ($p > 0.05$). While there was significant variability between individual neurons and across spatial locations for the same neuron (Fig. 3), on average, multisensory response latencies and discharge durations (53± 12 ms and 482± 125 ms, respectively) did not differ significantly from the predicted responses (49 ± 11 ms and 498 ± 134 ms, respectively) ($p > 0.05$).

The temporal response profiles of SC neurons recorded from DR+ animals differ significantly from those of NR SC neurons in a number of key dimensions. DR+ neurons were found to have significantly longer discharge durations ($p < 0.05$) (Fig. 4A), significantly higher peak firing rates ($p < 0.05$) (Fig. 4B), and significantly higher mean firing rates ($p < 0.05$) (Fig. 4C). Furthermore, DR+ neurons demonstrated an average level of spontaneous firing (54 ± 16 Hz) that was nearly an order of magnitude larger than the mean spontaneous firing rate of NR SC neurons (6 ± 4 Hz) (Fig. 4D). In contrast, multisensory stimulus evoked response latencies did not differ significantly across NR and DR+ neurons.

3.3. Influence of STRF heterogeneity on multisensory interactions

To facilitate comparisons of integrative capacity across conditions for individual neurons, the corresponding actual and predicted multisensory responses were aligned to a single time point – the onset of the predicted multisensory response. When viewed in this way, it was a common characteristic of individual multisensory SC neurons of NR animals to display significant multisensory interactions at various time points during the evoked response cycle. The typical temporal profile for these multisensory interactions is reflected well in the group data, with integration growing slowly throughout the course of the response (Fig. 5A). In contrast, significant superadditive and subadditive multisensory interactions were rarely observed in the responses of individual SC neurons of DR+ animals. This pattern is best illustrated when data from the entire population of SC neurons from DR+ animals is collapsed (Fig. 5B), highlighting the lack of any significant difference from the response predicted by simply summing the unisensory responses. In contrast, when the actual and predicted multisensory responses were aligned to the offset of the predicted multisensory response, similar patterns of integration emerged in both the NR and DR+ data sets (Fig. 5, right column).

4. Discussion

In the current study, we show that there appears to be a critical period for the development of a normal multisensory processing architecture in the cat superior colliculus (SC). Hence, animals raised in darkness and returned to normal lighting conditions as adults (i.e., DR+ animals) fail to develop the spatiotemporal receptive field (STRF) structure and integrative capacity that characterize animals raised under normal lighting conditions (i.e., NR animals). The difference between these populations manifested in a number of dimensions of the evoked multisensory responses (e.g., response mean, response duration, peak firing rate, etc.). Although the multisensory responses of SC neurons in both the NR and DR+ animals were significantly greater than their component visual and auditory responses, only the multisensory responses of SC neurons from NR animals showed a consistent pattern of deviating from the linear sum of these unisensory responses. Such a result suggests that visual experience during a critical period of postnatal life is essential for the development of the non-linear multisensory responses that characterize normal SC function, and that are likely derived from cortical projections that gate these integrative features (Harting et al., 1992; Jiang et al., 2001; Stein et al., 2002; Wallace et al., 1993; Wallace and Stein, 1994). These results are in strong accordance with prior work showing that binocular deprivation

results in significant changes in the sensory response profiles of SC neurons (Rauschecker and Harris 1983). Furthermore, this previous work was extended to implicate AES in the changes induced in the SC by visual deprivation (Rauschecker 1995). Future work will attempt to better characterize the critical period for these developmental events.

Along with the developmental and plasticity-related significance of this study, the work also represents the first description of the STRF organization of multisensory SC neurons in normal adults. Extending our prior work examining the STRF architecture of multisensory neurons in the anterior ectosylvian sulcus (AES) of the cat cortex (Royal et al., 2009), we have shown that the STRF architecture of NR multisensory SC neurons is equally complex, and reveals a temporal dynamism to the multisensory interactions exhibited by these neurons not previously appreciated. The most striking temporally-based difference in the response profiles of NR SC neurons was in the extended duration of the multisensory response when compared to a simple linear summation of the component unisensory responses. Such a prolongation of the multisensory response is likely to have profound consequences for the sensorimotor transformation performed by the SC, and for the behaviors that result from these processes. In contrast, the DR+ animals failed to show similar changes in response duration, a result that would be expected to have implications for SC-directed behaviors. Extended duration responses might play an important role in the behavioral enhancements seen in response to multisensory stimuli in a spatial localization setting (Stein et al., 1988; Stein et al., 1989).

Although outside of the evoked response domain, a related finding is likely to be the greatly amplified spontaneous activity that characterized the DR+ animals. The greatly enhanced basal activity profiles of these neurons are likely to reflect changes in inhibitory processes that normally keep SC spontaneous firing rates low (Hikosaka and Wurtz, 1983; Munoz et al., 1991; Munoz and Wurtz, 1995a, 1995b). Intriguingly, prior work has shown a strong relationship between spontaneous activity and integrative features of SC neurons (Perrault et al., 2003, 2005), with neurons exhibiting high spontaneous firing rates generally showing an absence of superadditive interactions. Hence, changes in inhibitory mechanisms brought about by dark-rearing may alter the dynamic range of SC neurons, with resultant effects on their integrative capacity.

As alluded to in the introduction, the nature of multisensory interactions has long been known to be dependent on a set of spatial, temporal and inverse effectiveness principles (Calvert, 2004; Meredith and Stein, 1986; Stein and Meredith, 1993). It is important to recognize that despite the utility of these principles, they often fail to fully characterize a given neuron’s integrative capacity. This is more than likely the result of the inherent interrelationship of these principles, in that space, time and effectiveness are highly interdependent dimensions. For example, a change in the spatial location of a multisensory stimulus complex often changes the magnitude of the evoked response because of the structural heterogeneities in the receptive field architecture. Because of these dependencies, the STRF construct offers more accurate insights into the complexity and dynamism of the multisensory processing architecture of SC neurons. In recent work, we have employed this same method of analysis to begin to examine multisensory neurons within the anterior ectosylvian sulcal (AES) cortex of the cat (Carriere et al., 2008). This work in cortex, coupled with the current study in the SC, represents the first view into how the domains of space and time interact in the generation of a multisensory neuron’s integrated responses. Perhaps most important in the current work is that despite exhibiting a striking and complex spatiotemporal response architecture, the multisensory interactions of SC neurons in normally-reared animals showed a consistent temporal “signature,” building slowly throughout the course of the entire response (Fig. 5); a pattern that is in stark contrast to the flat growth curve observed in the integrative capacities of DR+ multisensory neurons. These

findings are provocative in that they may offer new mechanistic insights into the development and maintenance of multisensory circuits and processes; insights that will likely be of great utility for the recent surge of interest in modeling multisensory interactions (Anastasio and Patton, 2003; Avillac et al., 2005; Diederich and Colonius, 2004; Rowland et al., 2007; Xing and Andersen, 2000).

The techniques used here to construct SRFs and STRFs represent simply a first approximation of the complexities inherent in the receptive field architecture of multisensory SC neurons. Indeed, future work will seek to build on this foundation by using more sophisticated methods and awake and behaving animals. Nonetheless, and despite these limitations, the current work provides a key set of insights into the relative contributions of sensory experience to the development of a multisensory neuron's response dynamics and integrative capacity, and extends previous work by showing that adult experience is not sufficient to reconstitute the normal response architecture of these neurons. In addition to its impact on multisensory processing, the current work highlights that early sensory experience plays an important role in determining key aspects of a multisensory neuron's response profile, including duration, peak firing rate, and mean response magnitude. Perhaps the most provocative difference was the finding that multisensory DR+ SC neurons had a significantly higher level of spontaneous activity than NR multisensory SC neurons. This result is especially noteworthy given its consistency with earlier work in AES (Carriere et al., 2007) that suggested that dark-rearing alters the normal balance of excitation and inhibition in cortical multisensory circuits. Future investigations will employ more sophisticated techniques (e.g., reverse correlation) to generate and analyze SRFs and STRFs, and will focus heavily on identifying the functional mechanisms underlying all of the significant differences that separate NR and DR+ spatiotemporal response dynamics, as well as the exact timeline of these developmental changes.

Acknowledgments

This work was supported by the National Institute of Mental Health Grant MH-63861 and by the Vanderbilt Kennedy Center for Research on Human Development. We would like to acknowledge the technical expertise of Zachary Barnett. We would also like to thank LuAnn Toy and Troy Apple, DVM for their expert assistance with animal care.

Abbreviations

AES	anterior ectosylvian sulcus
SRF	spatial receptive field
STRF	spatiotemporal receptive field
AEV	anterior ectosylvian visual area
SIV	fourth somatosensory cortex
FAES	auditory Field AES
SC	superior colliculus
SRF	spatial receptive field
RF	receptive field
kg	kilogram
mg	milligram
im	intramuscular

h	hour
iv	intravenous
LRS	lactated Ringer solution
ml	milliliter
PC	personal computer
Hz	Hertz
kHz	kilohertz
LED	light emitting diode
cd	candela
m	meter
cm	centimeter
ms	millisecond
dB	decibel
SPL	sound pressure level
fig	figure
M	multisensory
V	visual
A	auditory

References

Anastasio TJ, Patton PE. A two-stage unsupervised learning algorithm reproduces multisensory enhancement in a neural network model of the corticotectal system. J Neurosci. 2003; 23(17):6713–6727. [PubMed: 12890764]

Avillac M, Deneve S, Olivier E, Pouget A, Duhamel JR. Reference frames for representing visual and tactile locations in parietal cortex. Nat Neurosci. 2005; 8(7):941–949. [PubMed: 15951810]

Calvert, GA.; Spence, C.; Stein, BE. The Handbook of Multisensory Processes. Cambridge, MA: The MIT Press; 2004.

Carriere BN, Royal DW, Perrault TJ, Morrison SP, Vaughan JW, Stein BE, et al. Visual deprivation alters the development of cortical multisensory integration. J Neurophysiol. 2007; 98(5):2858–2867. [PubMed: 17728386]

Carriere BN, Royal DW, Wallace MT. Spatial heterogeneity of cortical receptive fields and its impact on multisensory interactions. J Neurophysiol. 2008; 99(5):2357–2368. [PubMed: 18287544]

Diederich A, Colonius H. Bimodal and trimodal multisensory enhancement: effects of stimulus onset and intensity on reaction time. Percept Psychophys. 2004; 66(8):1388–1404. [PubMed: 15813202]

Harting JK, Updyke BV, Van Lieshout DP. Corticotectal projections in the cat: anterograde transport studies of twenty-five cortical areas. J Comp Neurol. 1992; 324(3):379–414. [PubMed: 1401268]

Hikosaka O, Wurtz RH. Visual and oculomotor functions of monkey substantia nigra pars reticulata. IV. Relation of substantia nigra to superior colliculus. J Neurophysiol. 1983; 49(5):1285–1301. [PubMed: 6306173]

Jiang W, Wallace MT, Jiang H, Vaughan JW, Stein BE. Two cortical areas mediate multisensory integration in superior colliculus neurons. J Neurophysiol. 2001; 85(2):506–522. [PubMed: 11160489]

Kim HG, Connors BW. Apical dendrites of the neocortex: correlation between sodium- and calcium-dependent spiking and pyramidal cell morphology. J Neurosci. 1993; 13(12):5301–5311. [PubMed: 8254376]

Mason A, Nicoll A, Stratford K. Synaptic transmission between individual pyramidal neurons of the rat visual cortex *in vitro*. J Neurosci. 1991; 11(1):72–84. [PubMed: 1846012]

Meredith MA, Stein BE. Interactions among converging sensory inputs in the superior colliculus. Science. 1983; 221:389–391. [PubMed: 6867718]

Meredith MA, Stein BE. Visual, auditory, and somatosensory convergence on cells in superior colliculus results in multisensory integration. J Neurophysiol. 1986; 56(3):640–662. [PubMed: 3537225]

Munoz DP, Guitton D, Pelisson D. Control of orienting gaze shifts by the tectoreticulospinal system in the head-free cat. III. Spatiotemporal characteristics of phasic motor discharges. J Neurophysiol. 1991; 66(5):1642–1666. [PubMed: 1765799]

Munoz DP, Wurtz RH. Saccade-related activity in monkey superior colliculus.I Characteristics of burst and buildup cells. J Neurophysiol. 1995a; 73(6):2313–2333. [PubMed: 7666141]

Munoz DP, Wurtz RH. Saccade-related activity in monkey superior colliculus. II. Spread of activity during saccades. J Neurophysiol. 1995b; 73(6):2334–2348. [PubMed: 7666142]

Perrault TJ Jr, Vaughan JW, Stein BE, Wallace MT. Neuron-specific response characteristics predict the magnitude of multisensory integration. J Neurophysiol. 2003; 90(6):4022–4026. [PubMed: 12930816]

Perrault TJ Jr, Vaughan JW, Stein BE, Wallace MT. Superior colliculus neurons use distinct operational modes in the integration of multisensory stimuli. J Neurophysiol. 2005; 93(5):2575–2586. [PubMed: 15634709]

Rowland B, Stanford T, Stein B. A Bayesian model unifies multisensory spatial localization with the physiological properties of the superior colliculus. Exp Brain Res. 2007; 180(1):153–161. [PubMed: 17546470]

Royal DW, Carriere BN, Wallace MT. Cortical Multisensory Interactions. Exp Brain Res. 2009 (*accepted for publication*).

Sayer RJ, Friedlander MJ, Redman SJ. The time course and amplitude of EPSPs evoked at synapses between pairs of CA3/CA1 neurons in the hippocampal slice. J Neurosci. 1990; 10(3):826–836. [PubMed: 2319304]

Stanford TR, Quessy S, Stein BE. Evaluating the operations underlying multisensory integration in the cat superior colliculus. J Neurosci. 2005; 25(28):6499–6508. [PubMed: 16014711]

Stein BE, Huneycutt WS, Meredith MA. Neurons and behavior: the same rules of multisensory integration apply. Brain Res. 1988; 448(2):355–358. [PubMed: 3378157]

Stein, BE.; Meredith, MA. The Merging of the Senses. Cambridge, MA: MIT Press; 1993.

Stein BE, Meredith MA, Huneycutt WS, McDade L. Behavioral indices of multisensory integration: orientation to visual cues is affected by auditory stimuli. J Cogn Neurosci. 1989; 1(1):12–24. [PubMed: 23968407]

Stein BE, Wallace MT. Comparisons of cross-modality integration in midbrain and cortex. Prog Brain Res. 1996; 112:289–299. [PubMed: 8979836]

Stein BE, Wallace MW, Stanford TR, Jiang W. Cortex governs multisensory integration in the midbrain. Neuroscientist. 2002; 8(4):306–314. [PubMed: 12194499]

Wallace MT, Carriere BN, Perrault TJ Jr, Vaughan JW, Stein BE. The development of cortical multisensory integration. J Neurosci. 2006; 26(46):11844–11849. [PubMed: 17108157]

Wallace MT, McHaffie JG, Stein BE. Visual response properties and visuotopic representation in the newborn monkey superior colliculus. J Neurophysiol. 1997; 78(5):2732–2741. [PubMed: 9356422]

Wallace MT, Meredith MA, Stein BE. Integration of multiple sensory modalities in cat cortex. Exp Brain Res. 1992; 91(3):484–488. [PubMed: 1483520]

Wallace MT, Meredith MA, Stein BE. Converging influences from visual, auditory, and somatosensory cortices onto output neurons of the superior colliculus. J Neurophysiol. 1993; 69(6):1797–1809. [PubMed: 8350124]

Wallace MT, Meredith MA, Stein BE. Multisensory integration in the superior colliculus of the alert cat. J Neurophysiol. 1998; 80(2):1006–1010. [PubMed: 9705489]

Wallace MT, Perrault TJ Jr, Hairston WD, Stein BE. Visual experience is necessary for the development of multisensory integration. J Neurosci. 2004; 24(43):9580–9584. [PubMed: 15509745]

Wallace MT, Stein BE. Cross-modal synthesis in the midbrain depends on input from cortex. J Neurophysiol. 1994; 71(1):429–432. [PubMed: 8158240]

Wallace MT, Stein BE. Early experience determines how the senses will interact. J Neurophysiol. 2007; 97(1):921–926. [PubMed: 16914616]

Xing J, Andersen RA. Models of the posterior parietal cortex which perform multimodal integration and represent space in several coordinate frames. J Cogn Neurosci. 2000; 12(4):601–614. [PubMed: 10936913]

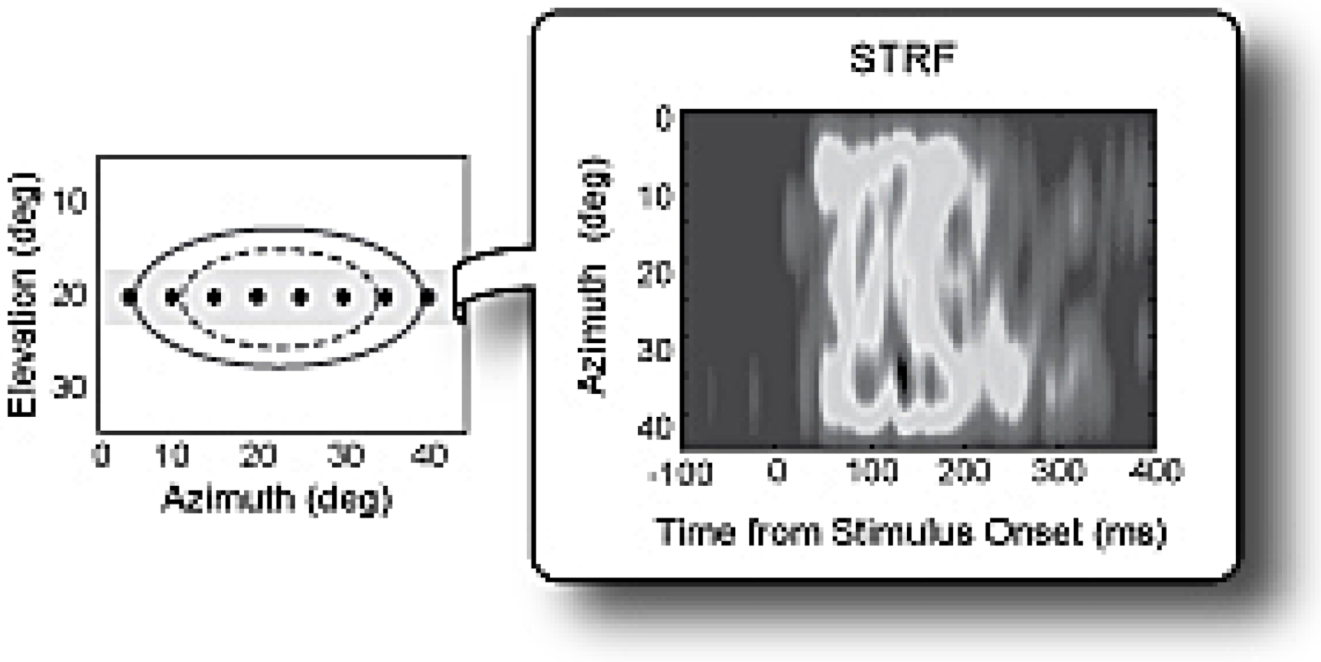

Fig. 1.

Construction of a spatiotemporal receptive field (STRF) for an individual SC neuron. On the left is shown the visual (dotted ellipse) and auditory (solid ellipse) receptive fields of a representative neuron and the stimulus locations (dots) used for creating the STRF. On the right is shown the STRF created for a single spatial plane (i.e., 20° elevation, shown on the left in the gray shading). In this plot the normalized evoked response (scaled to the maximal response) as a function of time (x-axis) and spatial location (y-axis) is represented in a pseudocolor format in which lighter shades of grey represent higher firing rates.

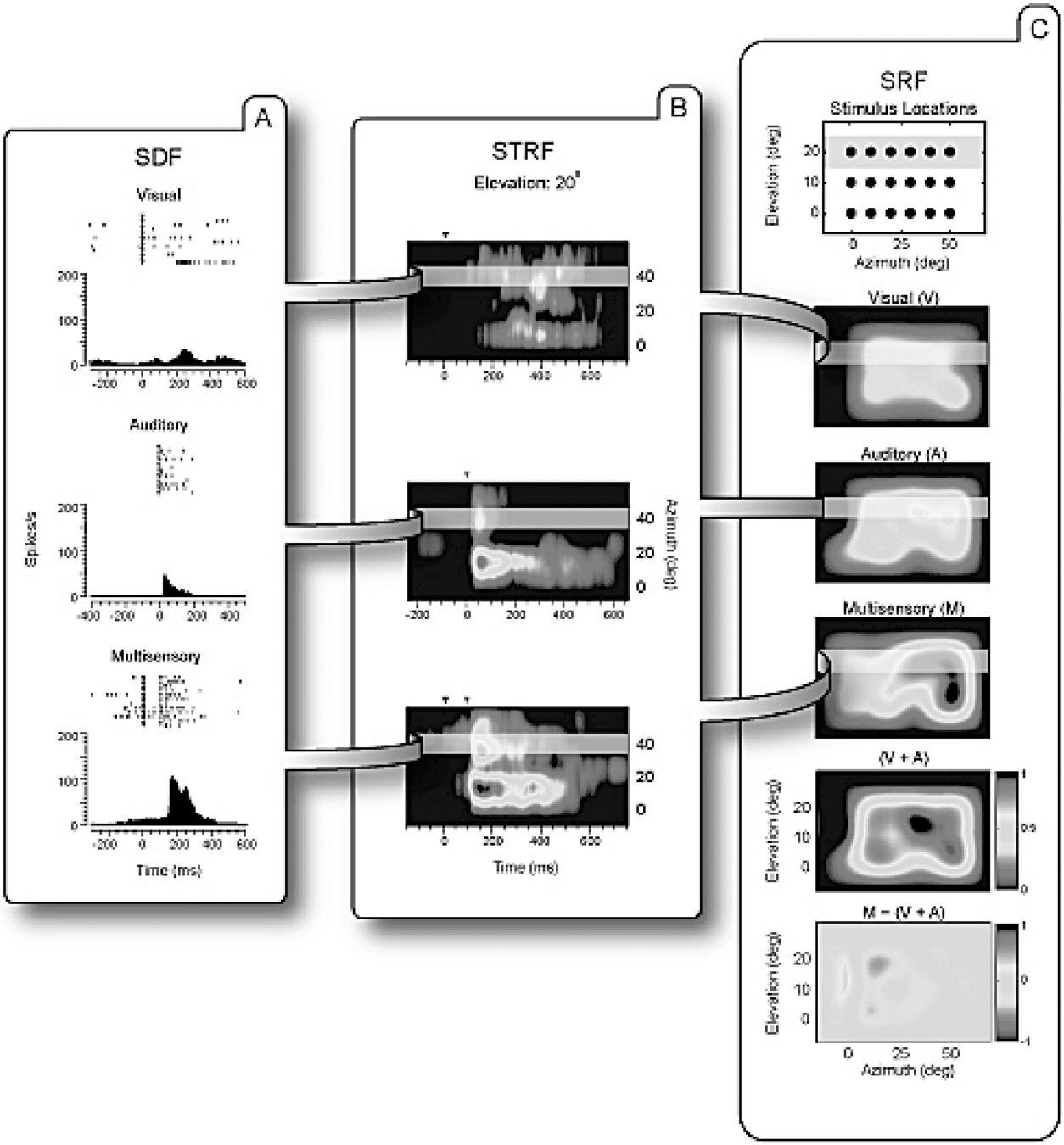

Fig. 2.

Representative example of spike density functions (SDFs), spatiotemporal receptive fields (STRFs), and spatial receptive fields (SRFs) for an SC neuron from a normally-reared (NR) animal. *A*: Rasters and SDFs illustrate this neuron's response to the visual, auditory and combined visual-auditory stimulus conditions. Triangles represent the onset of the visual (black) and auditory (grey) stimuli. *B*: The STRFs for the three stimulus conditions for the 20° elevation plane (see fig. 1 for a description of the construction of this representation). *C*: Top panel shows the stimulus locations (in two dimensions – azimuth and elevation) used for the construction of the SRF plots. Below this are shown the visual, auditory and multisensory SRFs for this neuron, along with that predicted from a simple summation of

the visual and auditory SRFs (V+ A) and a contrast plot showing the difference between the actual multisensory response and this prediction (M− [V+ A]). Note the areas of superadditive (darker shading) and subadditive (lighter shading) interactions in this contrast SRF.

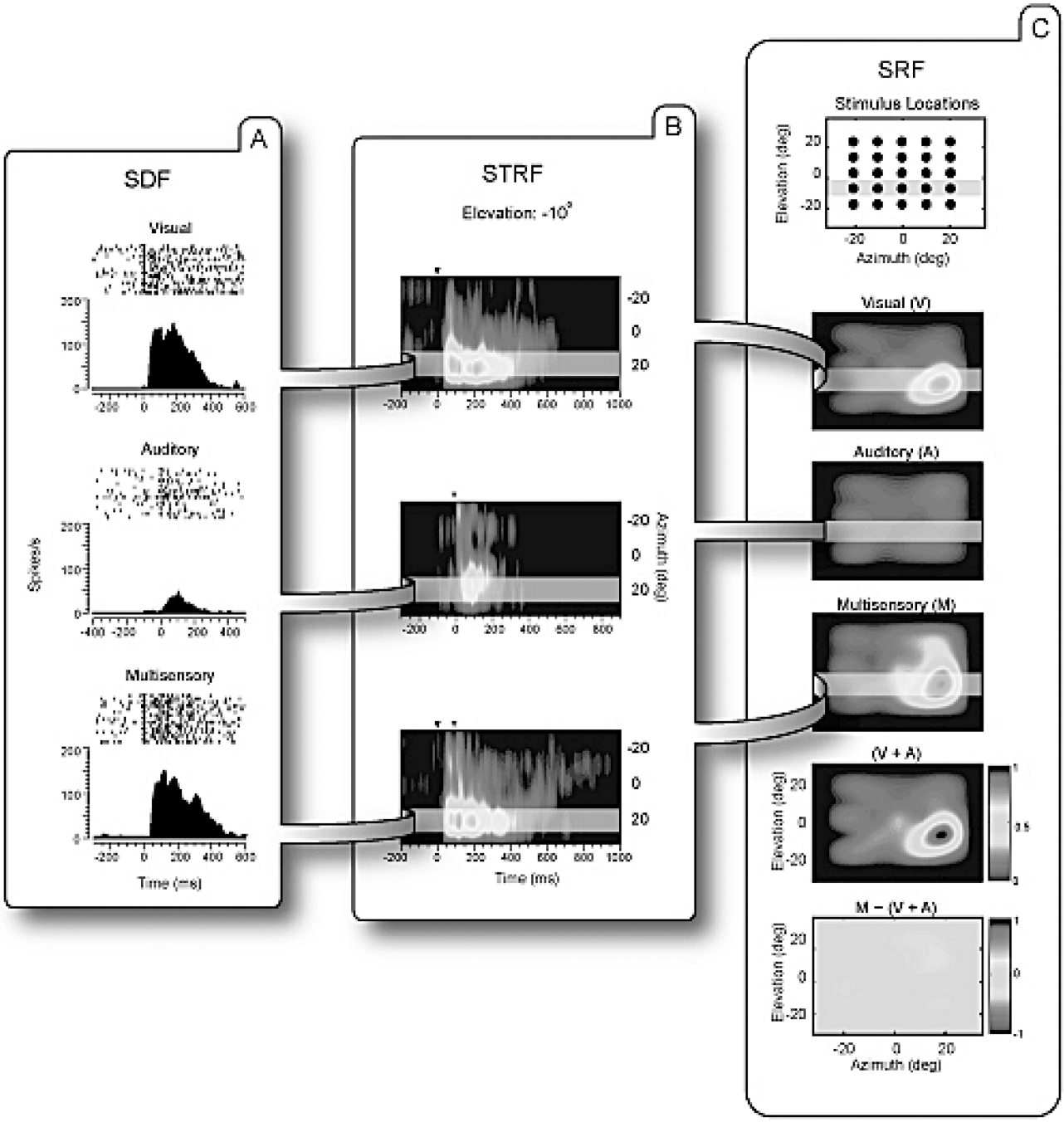

Fig. 3.

Representative example of spike density functions (SDFs), spatiotemporal receptive fields (STRFs), and spatial receptive fields (SRFs) for an SC neuron from a DR+ animal. Conventions are the same as for figure 2. Note in the SRF contrast plot (bottom right) that there is very little evidence for superadditive or subadditive multisensory interactions in this neuron.

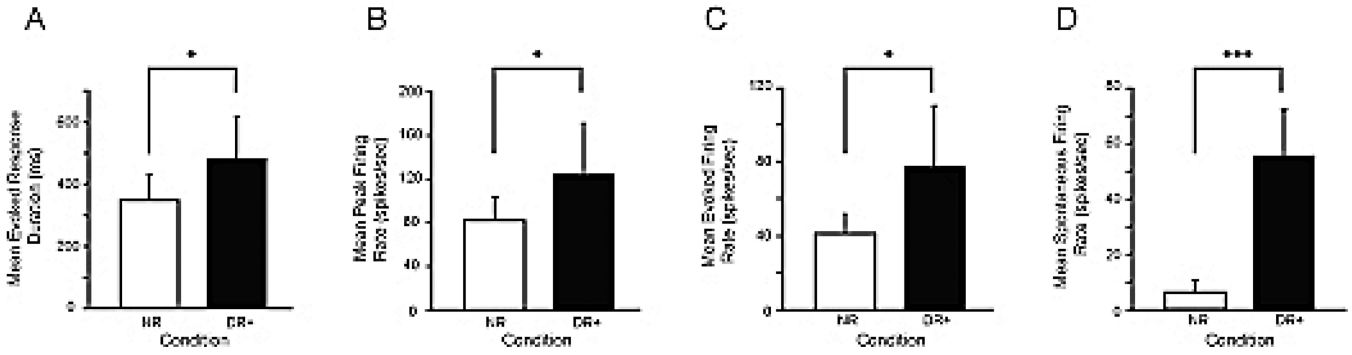

Fig. 4.

Comparison of multisensory stimulus evoked response dynamics between NR and DR+ populations. *A*: Mean evoked response duration. *B*: Mean peak firing rate. *C*: Mean evoked firing rate. *D*: Spontaneous firing rate.

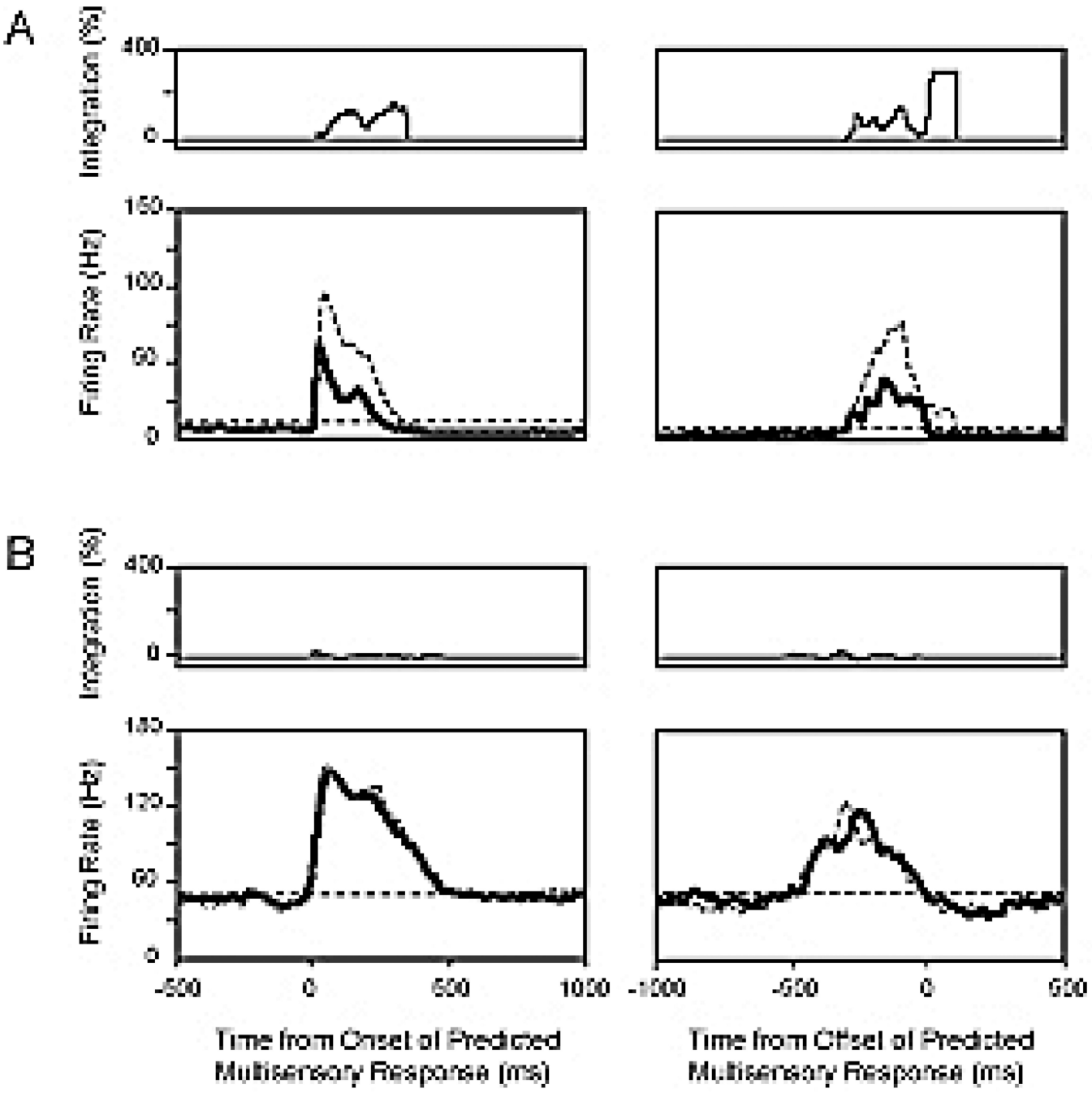

Fig. 5.

Comparison of temporal patterns of multisensory response and multisensory integration in relation to the onset and offset of the predicted multisensory response for the population of SC neurons from NR (A) and DR+ (B) animals. Whereas the *top panels* show changes in integrative capacity (%) as a function of time, the *bottom panels* depict changes in firing rate for the actual (dotted trace) and predicted (solid trace) multisensory conditions. Note that these responses are aligned to the predicted multisensory response's onset (left) and offset (right). This analysis emphasizes the lack of significant non-linearities in the responses of neurons from DR+ animals, in striking contrast to the condition in normal animals.